Donald L. Morton, Professor of Surgery and Chief, Divisions of Surgical Oncology and General Surgery, is a graduate of the University of California School of Medicine, San Francisco. As a young medical student at the University of California, he became interested in the newly emerging science of cancer, particularly in the clinical application of immunology to cancer treatment and diagnosis. Following his internship and residency, he joined the National Cancer Institute, Bethesda, MD, where he became Head of the Tumor Immunology Section and Senior Surgeon of the Surgery Branch. There, he performed extensive studies and developed his ideas of immunotherapy, and made a number of important contributions which helped advance the knowledge of the role of the immune system in the body's defense against cancer. In April, 1971, he came to UCLA and founded the Division of Surgical Oncology at the UCLA School of Medicine. Today, both the doctor and the Division are best known for work in the development and application of immunotherapy involving the stimulation of patients' immune responses as a treatment for cancer.

Dr. Morton is a recognized leader in the field of immunotherapy and has published almost 300 papers and articles advancing the knowledge of cancer, including malignant melanoma, lung cancer, bone and soft tissue sarcomas, breast cancer and colon cancer.

Heat Transfer in Surface-Cooled Objects Subject to Microwave Heating

KENNETH R. FOSTER, SENIOR MEMBER, IEEE, PORTONOVO S. AYYASWAMY, THIRUMALCHARI SUNDARARAJAN, AND KONERU RAMAKRISHNA

Abstract—**Several investigators in microwave bioeffects research have exposed biological preparations to intense microwave fields, while at the same time cooling the sample with flowing water. We examine the heat transfer characteristics of this situation, to estimate the maximum temperature increase and thermal time constants that might be encountered in such an experiment. The sample is modeled as a uniform sphere, cylinder, or slab subject to uniform heating, which is located in an unbounded coolant flow. The heat transfer is determined by the Biot and Reynolds numbers (which reflect the geometry, fluid flow, and material thermal properties of the system); the temperature rise is governed by the heat conduction equation coupled with external convection. The results are expressed in terms of nondimensional quantities, from which the thermal response of a heated object of arbitrary size can be determined. At low coolant flow rates, the maximum temperature rise can be biologically significant, even for relatively small objects (of millimeter radius) exposed to moderate levels of microwave energy (with a SAR of ca. 100 mW/g). The results are valid also where the coolant is a gas or a liquid different from water, the only restriction being on the Reynolds number of the flow.**

I. Nomenclature

- a Radius of the spherical tissue, in meters.
- B_n Constant of integration in (11), (18), and (25).
- Bi Biot number.
- C_p Specific heat, in joules per kilogram degrees Celsius.
- d Half the thickness of the rectangular tissue, in meters.
- h Convective heat transfer coefficient, in watts per square meter degrees Celsius.
- $J_m(x)$ Bessel function of the first kind and order m, of a real argument x.
- k Thermal conductivity, in watts per meter degrees Celsius; without subscript it refers to the tissue.
- L Characteristic length $= a$ or R or d or as appropriate.
- Nu Nusselt number $= hL/K$.
- Pe Peclet number $= \mathrm{Re}\,\mathrm{Pr}$.
- Pr Prandtl number $= \nu/\alpha$.
- Q Volumetric heat generation, in watts per cubic meter.
- r Radial coordinate.
- R Radius of the cylindrical tissue, in meters.
- Re Reynolds number $= U_\infty L/\nu$.
- t Time.
- T Temperature, in degrees Celsius.
- U_∞ Free stream velocity, in meters per hour.
- x Coordinate for rectangular slab tissue.

A. Greek Letters

- α Thermal diffusivity, in square meters per hour.
- θ Nondimensional temperature $= (T^* - T_0)/(QL^2/K)$.
- λ_n Eigenvalues defined by (13), (20), and (27).

Manuscript received December 16, 1981; revised March 22, 1982. This work was supported in part by the National Cancer Institute, Department of Health and Human Resources, under Grant 1-RO1-CA26046.

K. R. Foster is with the Department of Bioengineering, University of Pennsylvania, Philadelphia, PA 19104.

P. S. Ayyaswamy, T. Sundararajan, and K. Ramakrishna are with the Department of Mechanical Engineering and Applied Mechanics, University of Pennsylvania, Philadelphia, PA 19104.

0018-9480/82/0800-1158$00.75 ©1982 IEEE

ν Kinematic viscosity of the coolant, in square meters per hour.
ρ Density, in kilograms per cubic meter.
ψ Transient temperature response.

B. Subscripts

c Cooling period.
D Based on the diameter.
eq Equivalent.
f Coolant fluid.
max Maximum.
ss Steady-state.
0 Corresponding to $\mathrm{Re}=0$.
0 At $t=0$ or $r \to \infty$.

C. Superscripts

$*$ Dimensional quantity.
$\hat{}$ Of cylindrical object.
$\breve{}$ Of rectangular object.

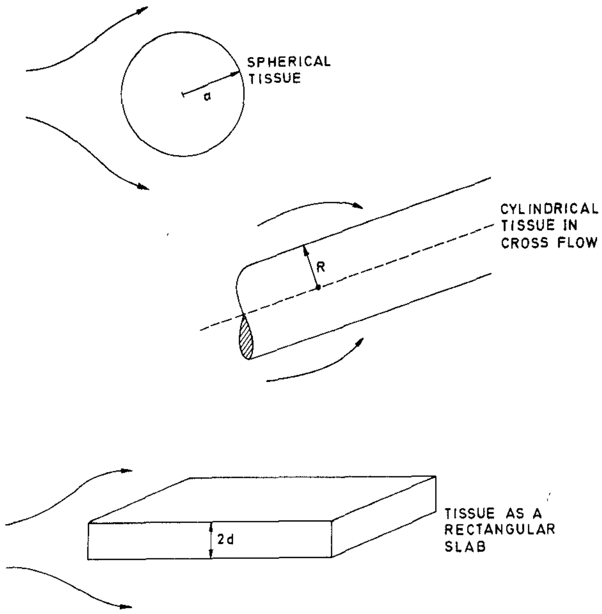

Fig. 1. Three tissue geometries considered in the analysis.

II. Introduction

IT IS WELL known that tissues, when exposed to microwave or radiowave heating, heat up as the electromagnetic energy is absorbed. An important problem in microwave bioeffects research is to distinguish between effects that are produced directly by the electromagnetic fields, and those that are a consequence of the heating alone. To address this problem, several experiments have been performed in which a small biological preparation (such as nerve bundle, eye lens, or a small pipette filled with a cellular suspension) is exposed to a relatively intense electromagnetic field (with time averaged Specific Absorption Rate (SAR) sometimes as high as 1.5 W/g) while being cooled with a flowing liquid on its outside surface [1]–[6]. Because of the critical dependence of the temperature on the heat transfer properties of the object and coolant, it is desirable to develop suitable theoretical models to describe the thermal characteristics of the situation. An appropriate model can be used to estimate the magnitude of the temperature increase that will occur in the heated preparation and can help in defining the flow properties required to obtain sufficient cooling. To our knowledge, no such model has previously been developed for this class of microwave bioeffects experiments.

In this study, we examine the thermal characteristics of a tissue, subject to uniform electromagnetic heating and convective cooling on the outside. The tissue geometry is modeled as a sphere, circular cylinder, or rectangular slab. We calculate the thermal response of the object by solving the governing nondimensional equation in closed form. The solutions we obtain are quite general, and apply to heated objects of arbitrary size and composition, immersed in a coolant which could be a gas or liquid with a large possible range of flow rates, the only restriction being on the Reynolds number of the flow. Also, we estimate the minimum rate of coolant flow that is required to produce optimal cooling of the tissue, and the variation in the temperature rise with coolant flow rate, at less than this minimum flow rate. A variational analysis of time dependent heating of irradiated tissue has recently been presented by Bardati [7]. However, our approach—obtaining exact solutions to simplified models—is likely to provide a good understanding of the heat transfer characteristics of the type of experiment considered here. The results have obvious application to other situations in which an object is subject to heating throughout its volume and to convective cooling.

III. Statement of the Problem

The schematic diagram and the coordinate system for the problem are illustrated in Fig. 1. A homogeneous object is located in an unbounded, laminar, coolant flow and is subject to uniform internal heating at a rate Q beginning at time $t=0$. In a real experiment, the object would be a small biological preparation and the cooling fluid would be water or Ringer's solution. Also, in a real situation, both the object and the coolant are simultaneously heated by the incident microwave energy to varying degrees and the coolant flow regime may not be laminar. The resultant mathematical problem in this latter case would be quite complex. We consider here instead a simpler case, in which the object alone is heated and it is immersed in a flowing fluid with uniform temperature T_0 at a large distance from the object. Furthermore, we assume that the coolant is in a thermal steady-state, even though the tissue temperature is time dependent. This is a reasonable first approximation to the real situation and the results are likely to approximate the results obtained from a more exact analysis.

IV. Analysis

We consider the tissue to be modeled as a sphere, a cylinder, or a rectangular slab. The tissue is initially at a uniform temperature T_0. The irradiation will cause a uniform volumetric heat generation in the tissue, which is cooled by a fluid flow over its exterior surface. For purposes of convenience, we shall discuss the three separate cases as follows.

A. Spherical Object

We consider a sphere of radius a that is initially at uniform temperature T_0, subject to uniform heating at rate Q beginning at time $t^*=0$. The governing equation for this case is

$$\frac{1}{r^{*2}}\frac{\partial}{\partial r^*}\left(r^{*2}\frac{\partial T^*}{\partial r^*}\right)+\frac{Q}{k}=\frac{1}{\alpha}\frac{\partial T^*}{\partial t^*},\qquad 0\leqslant r^*\leqslant a,\quad t^*>0 \tag{1}$$

where the symbols are defined in the Nomenclature.

Equation (1) is subject to the initial condition (hereafter referred to as IC)

$$t^*<0\qquad T^*(r^*,t^*)=T_0 \tag{2a}$$

and the boundary conditions (hereafter referred to as BC's)

$$t^*>0\qquad |T^*(r^*,t^*)|<\infty \tag{2b}$$

everywhere in the domain, and

$$-k\frac{\partial T^*}{\partial r^*}=h(T^*-T_0),\qquad \text{on } r^*=a. \tag{2c}$$

In (2c), h is the heat transfer coefficient at the surface of the object, and will be estimated in a later section. In (1) we have assumed purely radial conduction and constant transport properties. Equations (1) and (2) are normalized as follows: distances are normalized by a, temperatures by $(T^*-T_0)/(Qa^2/k)$, and time by a^2/α. Then the nondimensional formulation can be written as follows:

$$\frac{1}{r^2}\frac{\partial}{\partial r}\left(r^2\frac{\partial\theta}{\partial r}\right)+1=\frac{\partial\theta}{\partial t} \tag{3}$$

with IC

$$t<0\qquad \theta(r,t)=0 \tag{4a}$$

and BC's

$$t>0\qquad |\theta(r,t)|<\infty \tag{4b}$$

everywhere in the domain, and

$$\frac{\partial\theta}{\partial r}=-Bi\theta,\qquad \text{on } r=1. \tag{4c}$$

Here Bi is the Biot number (equal to ha/k) which is the ratio of the internal to external thermal resistance of the body.

Now we write

$$\theta(r,t)=\theta_{ss}(r)+\Psi(r,t) \tag{5}$$

where $\theta_{ss}(r)$ is the steady-state solution and $\Psi(r,t)$ is the transient response. Substitution of (5) into (3) and (4) leads to

$$\frac{1}{r^2}\frac{\partial}{\partial r}\left(r^2\frac{d\theta_{ss}}{dr}\right)+1=0 \tag{6}$$

with BC's

$$|\theta_{ss}(r)|<\infty \tag{7a}$$

everywhere in the domain, and

$$\frac{d\theta_{ss}}{dr}=-\mathrm{Bi}\,\theta_{ss},\qquad \text{on } r=1 \tag{7b}$$

and

$$\frac{1}{r^2}\frac{d}{dr}\left(r^2\frac{\partial\Psi}{\partial r}\right)=\frac{\partial\Psi}{\partial t} \tag{8}$$

with IC's

$$t<0\qquad \Psi(r,t)=-\theta_{ss}(r),\qquad 0\leqslant r\leqslant 1 \tag{9a}$$

and BC's

$$t>0\ |\Psi(r,t)|<\infty \tag{9b}$$

everywhere in the domain, and

$$\frac{\partial\Psi}{\partial r}=-\mathrm{Bi}\,\Psi,\qquad \text{on } r=1. \tag{9c}$$

The solution of (6) subject to conditions in (7) is

$$\theta_{ss}(r)=\frac{-r^2}{6}+\frac{1}{3\,\mathrm{Bi}}+\frac{1}{6} \tag{10}$$

and that of (8) and (9) is

$$\Psi(r,t)=\sum_{n=0}^{\infty}B_n\frac{\sin\lambda_n r}{r}e^{-\lambda_n^2 t}. \tag{11}$$

In (11), the constants B_n are given by

$$B_n=\frac{\dfrac{\sin\lambda_n}{3\lambda_n^2}+\dfrac{\cos\lambda_n}{\lambda_n^3}-\dfrac{\sin\lambda_n}{\lambda_n^4}+\dfrac{1}{3\,\mathrm{Bi}}\left[\dfrac{\cos\lambda_n}{\lambda_n}-\dfrac{\sin\lambda_n}{\lambda_n^2}\right]}{\left[\dfrac{1}{2}-\dfrac{\sin 2\lambda_n}{4\lambda_n}\right]}. \tag{12}$$

In the above, the eigenvalues λ_n are the roots of the characteristic equation

$$1-\lambda\cot\lambda=\mathrm{Bi}. \tag{13}$$

A concise listing of λ_n as functions of Bi is given by Myers [8].

When the object reaches a steady-state, the heating is discontinued and the preparation is allowed to cool. For this case, the governing differential equation is the same as (3), except that the heat generation term does not appear. The boundary conditions also have the same form as (4b,c). The initial conditions for the cooling case are

$$t<0\qquad \theta_c(r,t)=\theta_{ss}(r)$$

where the subscript c denotes cooling. It immediately follows that

$$\theta_c(r,t)=-\Psi(r,t).$$

B. Cylindrical Object

The cylindrical tissue is taken to experience a crossflow of the coolant. The circular cylinder is of radius R and is sufficiently long that the end effects are negligible. The heat flow is then in the radial direction only. The governing differential equation and the associated conditions are (in the nondimensional form)

$$\frac{1}{r}\frac{\partial}{\partial r}\left(r\frac{\partial\hat{\theta}}{\partial r}\right)+1=\frac{\partial\hat{\theta}}{\partial t}, \qquad t>0, \qquad 0\leqslant r\leqslant 1 \qquad (14)$$

with IC

$$t<0 \qquad \hat{\theta}(r,t)=0 \qquad (15a)$$

and BC's,

$$|\hat{\theta}(r,t)|<\infty \qquad (15b)$$

everywhere in the domain, and

$$\frac{\partial\hat{\theta}}{\partial r}=-\widehat{\mathrm{Bi}}\,\hat{\theta}, \qquad \text{on } r=1. \qquad (15c)$$

In the above, $\hat{\theta}$ is the nondimensional temperature equal to $(T^*-T_0)/(QR^2/k)$, the radial distance is normalized by R, the time by R^2/α, and $\mathrm{Bi}\equiv(\hat{h}R/k)$. The carat ($\hat{}$) is used to indicate cylindrical geometry. Following a procedure similar to the spherical case, we let

$$\hat{\theta}(r,t)=\hat{\theta}_{ss}(r)+\hat{\Psi}(r,t) \qquad (16)$$

where

$$\hat{\theta}_{ss}(r)=\frac{-r^2}{4}+\frac{1}{2\widehat{\mathrm{Bi}}}+\frac{1}{4} \qquad (17)$$

is the steady-state solution, and

$$\hat{\Psi}(r,t)=\sum_{n=0}^{\infty}\hat{B}_nJ_0(\lambda_nr)e^{-\lambda_n^2t} \qquad (18)$$

is the transient response. $\hat{B}_n$ can be determined as

$$\hat{B}_n=-\frac{[\mathrm{Bi}\,J_2(\lambda_n)+\lambda_nJ_1(\lambda_n)]}{\widehat{\mathrm{Bi}}\,\lambda_n^2[J_0^2(\lambda_n)+J_1^2(\lambda_n)]}. \qquad (19)$$

The eigenvalues λ_n are the roots of the characteristic equation

$$\lambda J_1(\lambda)=\widehat{\mathrm{Bi}}\,J_0(\lambda) \qquad (20)$$

where $J_m(X)$ are the Bessel functions of the first kind and order m. The eigenvalues λ_n are also given in [8].

When the steady-state is reached, the tissue is allowed to cool. For the cooling case, the temperature distribution is given by

$$\hat{\theta}_c(r,t)=-\hat{\Psi}(r,t).$$

C. Rectangular Slab

We shall consider a finite slab of thickness $2d$ and lateral dimensions which are large compared to the thickness, so that the gradients in those directions are negligible. We will only solve the heat transfer equation in one dimension, but employ a three-dimensional model to estimate the heat transfer coefficient $\tilde{h}$. The midplane between the two faces (top and bottom) is then considered as an adiabatic surface. The nondimensional governing differential equation and the associated conditions are

$$\frac{\partial^2\tilde{\theta}}{\partial x^2}+1=\frac{\partial\tilde{\theta}}{\partial t} \qquad (21)$$

with IC

$$t<0 \qquad \tilde{\theta}(x,t)=0 \qquad (22a)$$

and BC's

$$t>0 \qquad \frac{\partial\tilde{\theta}}{\partial x}=0, \qquad \text{at } x=0 \qquad (22b)$$

$$\frac{\partial\tilde{\theta}}{\partial x}=-\tilde{\mathrm{Bi}}\,\tilde{\theta}, \qquad \text{at } x=1. \qquad (22c)$$

Here $x=x^*/d$ and $\tilde{\mathrm{Bi}}=\tilde{h}d/k$. The tilde ($\tilde{}$) is used to indicate the rectangular geometry. We write

$$\tilde{\theta}(x,t)=\tilde{\theta}_{ss}(x)+\tilde{\Psi}(x,t) \qquad (23)$$

where $\tilde{\theta}_{ss}(x)$ and $\tilde{\Psi}(x,t)$ can be shown to be

$$\tilde{\theta}_{ss}(x)=-\frac{1}{2}x^2+\frac{1}{2}+\frac{1}{\tilde{\mathrm{Bi}}} \qquad (24)$$

and

$$\tilde{\Psi}(x,t)=\sum_{n=0}^{\infty}\tilde{B}_n\cos\lambda_nxe^{-\lambda_n^2t}. \qquad (25)$$

The coefficients $\tilde{B}_n$ and $\tilde{\lambda}_n$ in (25) are determined from

$$\tilde{B}_n=\frac{\left[\frac{\sin\lambda_n}{2\lambda_n}+\frac{\cos\lambda_n}{\lambda_n^2}-\frac{\sin\lambda_n}{\lambda_n^3}\right]}{\left[\frac{1}{2}+\frac{1}{4}\frac{\sin 2\lambda_n}{\lambda_n}\right]} \qquad (26)$$

and

$$\lambda\tan\lambda=\tilde{\mathrm{Bi}}. \qquad (27)$$

For the cooling case

$$\tilde{\theta}_c(x,t)=-\tilde{\Psi}(x,t). \qquad (28)$$

V. Evaluation of the Heat Transfer Coefficients

The heat transfer coefficients h used in the definitions of Bi, $\widehat{\mathrm{Bi}}$, and $\tilde{\mathrm{Bi}}$ are evaluated from the steady-state Nusselt number correlations available in the heat transfer literature. These correlations summarize experimental data over very wide ranges of experimental conditions, and reflect the thermal and hydrodynamic properties of the coolant flow. Therefore, the present results can be applied to cases in which the coolant is a liquid other than water, or even a gas, the only restriction being on the Reynolds number of flow. The evaluation we make is consistent with the assumption of quasi-steady-state of the coolant heat transfer. The calculation of the heat transfer itself will be made on the basis of the temperature difference between the tissue surface and the bulk temperature of the coolant.

1) For a spherical object, the following correlation is taken from Gebhart (9):

$$\mathrm{Nu}_D=\frac{2ha}{k_f}=2.0+0.6\,\mathrm{Re}_D^{1/2}\mathrm{Pr}^{1/3}, \qquad \text{for } 1<\mathrm{Re}_D<7\times10^4. \qquad (29)$$

Here Nu_D and Re_D are, respectively, the Nusselt and Reynolds numbers which are based on the diameter of the sphere (cf. Nomenclature), and Pr is the Prandtl number of the coolant. The constant 2.0 in (29) is the Nusselt number for a stagnant coolant bounding the sphere ($\mathrm{Re}_D=0$).

2) For a cylindrical object, the following correlation suggested by Churchill and Bernstein (10) is used:

$$\hat{\mathrm{Nu}}_D = \frac{2\hat{h}R}{k_f} = 0.3 + \frac{0.62\,\hat{\mathrm{Re}}_D^{1/2}\,\mathrm{Pr}^{1/3}}{\left[1+\left(\frac{0.4}{\mathrm{Pr}}\right)^{2/3}\right]^{1/4}} \tag{30}$$

for $0.04 < \hat{\mathrm{Re}}_D < 4000$. Again, $\hat{\mathrm{Nu}}_D$ and $\hat{\mathrm{Re}}_D$ are based on the cylinder diameter.

3) For a rectangular slab of finite thickness there are no correlations that are available in published literature. A general solution to this problem is quite difficult; even to experimentally determine a suitable heat transfer correlation for the flow past a heated, finite thickness, finite slab, the task is formidable. Instead, it is customary to approximate the problem by making suitable assumptions. In this paper we set

$$\tilde{\mathrm{Nu}}_{D_{\mathrm{eq}}} = \frac{\tilde{h}D_{\mathrm{eq}}}{k_f} = \tilde{\mathrm{Nu}}_{\mathrm{conduction}} + \tilde{\mathrm{Nu}}_{\mathrm{convection}}. \tag{31}$$

The $\tilde{\mathrm{Nu}}_{\mathrm{conduction}}$ is evaluated by approximating the rectangular slab as a solid bounded by two circular disks, one at the top and the other at the bottom. The total surface area of the disk will equal the surface area of the slab. The analytical solution to the heat conduction problem of a circular disk in a stagnant fluid is given by Carslaw and Jaegar [11]. From this, it follows that, for our problem

$$\tilde{\mathrm{Nu}}_{\mathrm{conduction}} \cong \frac{4}{\sqrt{\pi}} = \frac{2\tilde{h}R_{\mathrm{eq}}}{k} \tag{32}$$

where R_{eq} is the radius of the equivalent circular disk. Next, the $\tilde{\mathrm{Nu}}_{\mathrm{convection}}$ is evaluated on the assumption that the slab could be replaced by an equivalent sphere. Then we can write

$$\tilde{\mathrm{Nu}}_{\mathrm{convection}} = \frac{\tilde{h}D_{\mathrm{eq}}}{k_f} = 0.6\,\tilde{\mathrm{Re}}_{D_{\mathrm{eq}}}^{1/2}\,\mathrm{Pr}^{1/3}. \tag{33}$$

In (33), D_{eq} is the diameter of an equivalent sphere whose surface area equals the surface area of the slab.

Since we have developed an expression for the $\tilde{\mathrm{Nu}}$ on an approximate basis, it is worthwhile to examine the validity or appropriateness of the results obtained. In this context, Brenner [12] has published solutions to the heat transfer problem of flow past an arbitrarily shaped body. His solutions are limited to the range of low Peclet numbers ($\mathrm{Pe} = \mathrm{Pr} \cdot \mathrm{Re}$). Brenner's analysis is by asymptotic methods and he offers the result for $\mathrm{Pe} < 1$

$$\frac{\mathrm{Nu}}{\mathrm{Nu}_0} = 1 + \frac{\mathrm{Nu}_0 \mathrm{Pe}}{8} + 0(\mathrm{Pe}^2) \tag{34}$$

where Nu_0 is the Nusselt number for the stagnant fluid case. In (34), the characteristic length is the largest length of the arbitrarily shaped body. For a sphere, this would be the diameter, and for a rectangular slab this would be the principal diagonal. Brenner's equation will be used as a check on the correlations employed in our paper, in the next section.

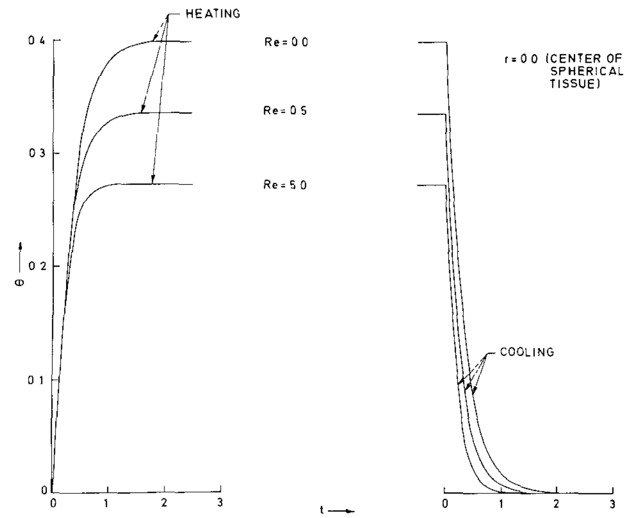

Fig 2. Nondimensional temperature (θ) versus time (t) at the center of the tissue sphere, for coolant flow rates with Reynolds numbers of 0, 0.5, and 5.0.

VI. Results and Discussion

The transient temperature distributions during the heat up and cooling of a spherical, a cylindrical, and a rectangular slab tissue are calculated for different flow Reynolds numbers. In these calculations we have used the following values for the tissue properties:

$$\text{density:}\quad \rho_{\mathrm{tissue}} = \rho_{\mathrm{water}}$$
$$\text{thermal conductivity:}\quad k_{\mathrm{tissue}} = 0.7k_{\mathrm{water}}$$
$$\text{specific heat:}\quad C_{p_{\mathrm{tissue}}} = 0.7C_{p_{\mathrm{water}}}.$$

The properties are evaluated at a temperature $T_0 = 30°\mathrm{C}$.

Fig. 2 shows the nondimensional temperature θ versus nondimensional time t, at the center $r = 0$ of a spherical tissue for $\mathrm{Re}_D = 0$, 0.5, and 5. At any given time t, the maximum temperature occurs at the center of the sphere; the maximum value is attained during the steady-state of the heating period. The nondimensional, maximum temperature at the center of the sphere, in the steady-state, follows from (10) to be

$$\theta_{\max} = \frac{1}{6} + \frac{1}{3\,\mathrm{Bi}}. \tag{35}$$

It is seen from (35) that the maximum temperature attained decreases with increasing Reynolds numbers, which is an expected consequence of the higher rate of heat removal from the surface of the tissue. However, for Reynolds numbers greater than about 5, the maximum temperature very quickly approaches its limiting value of 1/6. This behavior is evident from Fig. 2. It is also observed from Fig. 2 that the steady-state is attained faster with increasing Reynolds number. The time taken to attain a steady-state is determined by the time constants of the problem, which appear as eigenvalues in (11), (18), and (25). A high Re results in a high Bi and the associated eigenvalues are large [8]. For objects with comparable characteristic dimensions (a, R, d), these eigenvalues increase in the following order: slab, cylinder, and sphere. (This is not surprising in view of the greatly different

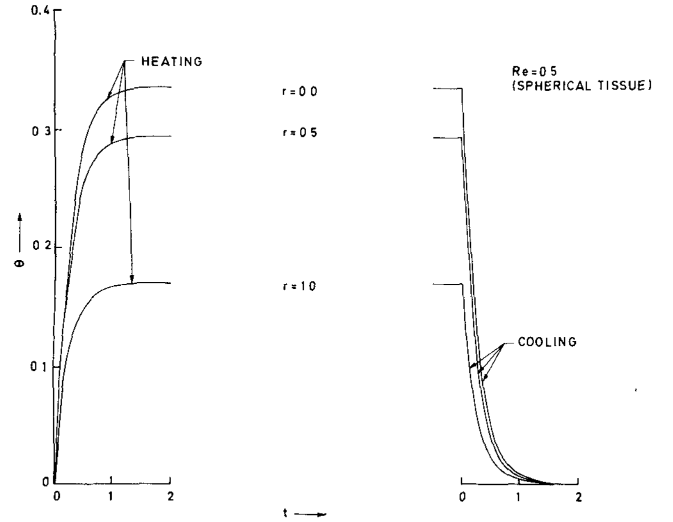

Fig. 3. Nondimensional temperature (θ) versus nondimensional time (t) at different radial locations in the tissue sphere, assuming a coolant flow with Reynolds number 0.5. The radius of the sphere is 1 in nondimensional units.

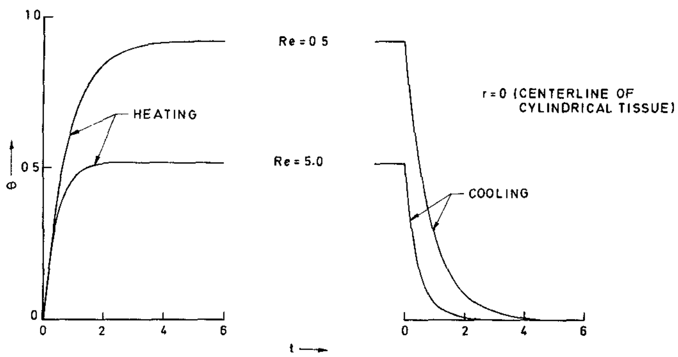

Fig. 4. Nondimensional temperature (θ) versus nondimensional time (t) on the centerline of a cylindrical object, for coolant flows with Reynolds numbers 0.5 and 5.0.

surface to volume ratios of these objects.) In each case, the lowest eigenvalue dominates, and the approach to the steady-state resembles an exponential process.

Fig. 3 shows the nondimensional temperature θ versus dimensionless time t for the spherical tissue. The Re is fixed at 0.5 and the values are given for three different radial locations $r = 0$, 0.5, and 1.0. All the curves in Fig. 3 correspond to the same set of time constants. Thus the time taken to reach steady-state is the same for all radial locations. At any time t, during heating or cooling, the temperature θ is higher as we move towards the center of the sphere. Since the time taken to attain the steady-state is independent of the radial location, the heating or cooling rate (temperature change/time) is higher as we approach the center.

Fig. 4 shows the nondimensional temperature θ versus time t at the center, $r = 0$, of a cylindrical tissue. The results are for $\hat{\mathrm{Re}}_D = 0.5$ and 5. There is no curve corresponding to $\hat{\mathrm{Re}}_D = 0$ because for an infinitely long cylinder with stagnant fluid on the outside, no steady-state solution exists [9]. The heating and cooling curves are similar to those found for the sphere, except that the time constants

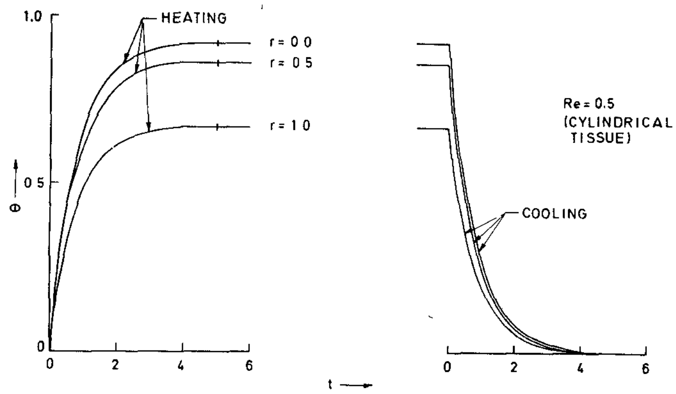

Fig. 5. Nondimensional temperature (θ) versus nondimensional time (t) for different radial locations in the cylindrical tissue, for coolant flow with a Reynolds number of 0.5. The diameter of the cylinder is 1 in nondimensional units.

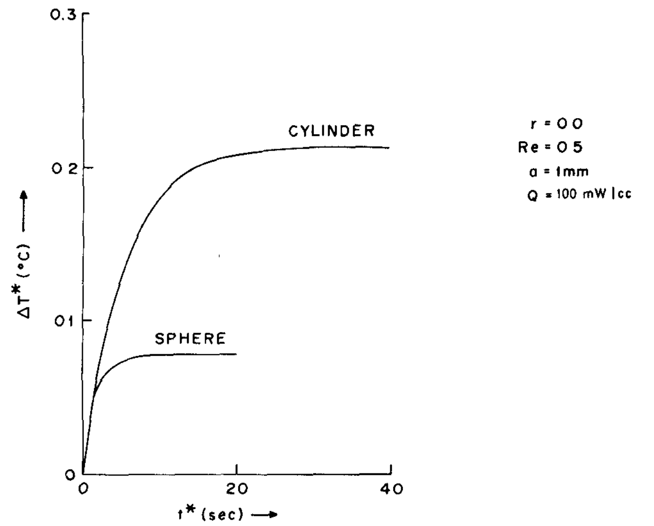

Fig. 6. Dimensional temperature (in degrees Celsius) versus dimensional time (in seconds) at the center of a heated tissue cylinder and sphere, assuming a heating rate Q of 100 mW/cm^3, and a Reynolds number of flow of the coolant of 0.5.

are larger. Fig. 5 shows the variation of θ with t at $\mathrm{Re} = 0.5$ and at three radial locations $r = 0$, 0.5, and 1.0. Also, the nondimensional temperature levels attained for a cylindrical tissue are higher than those for an equivalent spherical tissue, as expected because a cylindrical object has lesser surface area for heat transfer per unit volume compared to an equivalent spherical object. Fig. 6 offers a comparison between the dimensional temperature at the center that is attained in a cylinder and a sphere for the same heat generation of $Q = 100$ mW/cm^3. The Re_D for the external flow is fixed at 0.5. The tissue dimensions are $a = R = 1$ mm.

Fig. 7 shows the variation of θ with t, at the midplane of a rectangular slab of tissue. The $\widetilde{\mathrm{Re}}_{D_{\mathrm{eq}}}$ values studied are 0.5 and 5. The tissue dimensions are taken to be 1 cm$\times$1 cm$\times$0.2 cm. The slab has the longest thermal response time, for equivalent size structure, of the three different geometries investigated in this paper. As mentioned earlier, we choose to compare our results with those of Brenner [12], which are applicable for the cases where $\mathrm{Pe} < 1$. In our problem, $\mathrm{Pr} \sim 5$. Therefore, a meaningful comparison

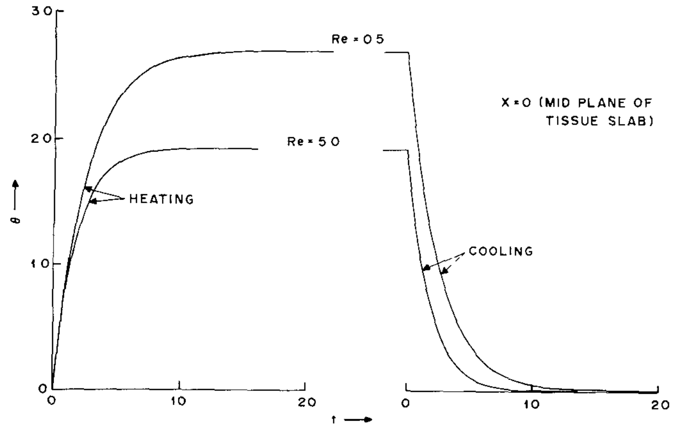

Fig. 7. Nondimensional temperature (θ) versus nondimensional time (t) in the midplane of a tissue slab, assuming Reynolds numbers of the coolant flow of 0.5 and 5.0.

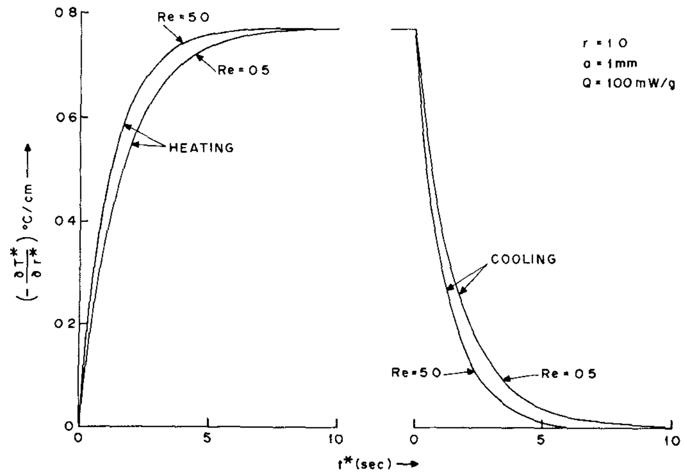

Fig. 8. The maximum temperature gradient, in degrees Celsius per centimeter at the surface of the tissue sphere, for two different Reynolds numbers.

TABLE I
COMPARISON OF NUSSELT NUMBERS

	Sphere	Rectangular Slab
Brenner's Eq. (Ref.12)	2.320	2.602
This Study	2.271	2.590

may be made for Re $\sim$ 0.1. Such a comparison turns out to be remarkably good (Table I).

Fig. 8 shows the dimensional radial temperature gradient (°C/cm) versus time (seconds), evaluated at the surface of a spherical tissue (where the gradient is a maximum). The Re_D studied are 0.5 and 5. The steady-state value for the dimensional temperature gradient is seen to be independent of the Reynolds number of the external flow. This value may be shown from the theory to be

$$\left.\frac{\partial T^*}{\partial r^*}\right|_{\text{surface}} = \frac{-Qa}{3k}. \tag{36}$$

VII. CONCLUDING REMARKS

From these results, several conclusions can be drawn that are important for the kind of experiment under consideration.

1) There is a minimum Reynolds number of coolant flow required for optimum cooling. In general, for an object of a given size heated at a given SAR, higher flow velocities of the coolant will result in lower steady-state temperature increases within the object. However, beyond a certain Reynolds number (which depends on the geometry of the object) no significant decreases are obtained; the temperature at the surface approaches that of the coolant, and the

temperature rise within the object is determined principally by its thermal conductivity. In an actual experiment, it is important to employ coolant flows with Reynolds numbers sufficiently high that the temperature increases in the object are at a minimum and the variations in temperature rise with (perhaps inadvertent) variations in flow rate are negligible.

The Reynolds number of coolant flow required to produce this optimum cooling can be easily obtained. We define a "transition" Reynolds number corresponding to a case where the temperature increase at the center of the object is 10 percent above that obtained in the limit of high coolant flow rate. We find

$$\text{Sphere:}\quad \mathrm{Re}_{D_{\text{transition}}} \simeq 4500\,(k/k_f)^2\mathrm{Pr}^{-2/3}$$

$$\text{Cylinder:}\quad \widehat{\mathrm{Re}}_{D_{\text{transition}}} \simeq 4200\,(k/k_f)^2\mathrm{Pr}^{-2/3}$$

$$\text{Slab:}\quad \widetilde{\mathrm{Re}}_{D_{\text{transition}}} \simeq 1100\left(\frac{k}{k_f}\frac{D_{\text{eq}}}{d}\right)^2\mathrm{Pr}^{-2/3} \quad (37)$$

for moderate to large Prandtl numbers ($\mathrm{Pr}>1$). For water flow past a tissue sphere, this transition Reynolds number is about 700. For a tissue sphere of radius 1 cm, this condition corresponds to a water flow velocity of 2.5 cm/s; for a 1-mm radius sphere, it would be tenfold higher. Because of the simplifications employed in these calculations, somewhat higher flow rates should be provided in an actual experiment to ensure optimum cooling.

2) The maximum temperature difference that can be established in a tissue subjected to uniform heating is bounded by the following limits:

$$\text{Sphere:}\quad \frac{Qa^2}{6k} \leqslant (T^*-T_0)_{\max} \leqslant \frac{Qa^2}{6k}\left(1+\frac{2k}{k_f}\right) \quad (38)$$

$$\text{Cylinder:}\quad \frac{QR^2}{4k} \leqslant (T^*-T_0)_{\max} \quad (39)$$

$$\text{Slab:}\quad \frac{Qd^2}{2k} \leqslant (T^*-T_0)_{\max} \leqslant \frac{Qd^2}{2k}\left\{1+0.89\,\frac{k}{k_f}\frac{D_{\text{eq}}}{d}\right\}. \quad (40)$$

For a tissue sphere of 1-cm radius whose material thermal properties are as given above, subject to a time-averaged SAR of 0.1 W/cm^3, the maximum temperature rise at the center is thus within the range of 3.9–9.3°C. For a 1-mm radius sphere subject to the same SAR, the comparable range is 0.04–0.1°C. Since these temperature increases are quite nonuniform throughout the preparation, they might elicit biological effects that are not observed in the simple control experiment of increasing the temperature of the bath, with no heating by microwave energy. Because of the quadratic dependence of the maximum temperature rise on the dimension of the object, the temperature rise in objects of less than millimeter dimension will be very small for any experimentally reasonable value of the SAR. This suggests the impossibility of producing biologically significant temperature gradients over cellular or macromolecular distances, even though tissue structures or macromolecules of these small dimensions might, under appropriate circumstances, absorb more electromagnetic energy per unit volume than its surroundings [13]–[15].

3) The thermal time constant, required for the sphere to reach the steady-state after the heating is begun, is of the order of a^2/α. For a tissue sphere of 1-cm radius, this is several minutes; for a 1-mm radius sphere, the time constant is reduced to a few seconds.

It is interesting to examine some of the previous bioeffects experiments in view of the present results. Chou and Guy [1] exposed isolated rabbit nerve bundles to microwave fields with an estimated SAR of 1.5 W/g. The changes they observed in the conduction velocity of these bundles corresponded to a 1° increase in the temperature of the preparation, which was equal to the measured increase in temperature of the coolant fluid during the exposure. From (39), we expect that the maximum temperature rise in the tissue was about 0.9°C (for a 1-mm radius nerve subject to maximum external cooling). It appears that, in this case, the differential heating of the nerve preparation could be significant, although the analysis of the investigators suggests that the tissue temperature for the most part was close to that of the coolant.

In contrast, in the experiments of Stewart–Dehann *et al.* [6], rat ocular lenses were exposed to microwave fields with SAR values in the range 120–1200 mW/cm^3. Assuming the diameter of the lens to be 0.7 cm, we estimate that the maximum temperature increase is in the range 0.6–6°C with optimum surface cooling, and up to threefold higher with less effective cooling. In producing the observed biological responses (local tissue damage through the lens), heating effects were probably significant, although the different effects produced by pulsed versus continuous-wave microwave energy with the same time-averaged SAR cannot be accounted for by this model.

Acknowledgment

We thank one of the referees from the National Cancer Institute, Department of Health and Human Resources, for helpful comments about earlier versions of the manuscript.

References

[1] C.-K. Chou and A. W. Guy, "Effects of electromagnetic fields on isolated nerve and muscle preparation," *IEEE Trans. Microwave Theory Tech.*, vol. MTT-26, pp. 141–147, Mar. 1978.

[2] K.-C. Chen and C.-J. Lin, "A system for studying effects of microwaves on cells in culture," *J. Microwave Power*, vol. 13, pp. 251–256, 1978.

[3] J. R. Rabinowitz, R. B. Olcerst, and W. W. Mumford, "The description of a system to irradiate cells in culture with microwaves," in *Proc. Symp. Biol. Effects Measurements Radiofrequency/Microwaves*, (Rockville, MD), Feb. 16–18, 1977, pp. 216–229.

[4] D. I. McRee, "Microwave Effects on Nerve Vitality," in *Abstracts 1977 Int. Symp. Biological Effects Electromagnetic Waves*, (Int. Union Radio Sci., Airlie, VA), Oct. 30–Nov. 4, 1977, p. 96.

[5] P. V. K. Brown and L. E. Larsen, "Differing effects of pulsed and CW microwave energy on nerve function as detected by birefringence measurement," *IEEE Trans. Microwave Theory Tech.*, vol. MTT-28, pp 1126–1133, 1980.

[6] P. J. Stewart-De Haan, M. O. Creighton, L. E. Larsen, J. H. Jacobi, W. M. Ross, and J. R. Trevithick, "Microwave and temperature effects on the murine ocular lens *in vitro*," in *Proc. 1980 IEEE MTT-S Int. Symp.*, pp. 341–344, 1980.
[7] F. Bardati, "Time dependent microwave heating and surface cooling of living tissues," *IEEE Trans. Microwave Theory Tech.*, vol. MTT-29, pp. 825–827, 1981.
[8] G. E. Myers, *Analytical Methods in Conduction Heat Transfer.* New York:McGraw-Hill, 1971.
[9] B. Gebhart, *Heat Transfer*, 2nd ed. New York:McGraw-Hill, 1971.
[10] S. W. Churchill and M. Bernstein, "A correlating equation for forced convection from gases and liquids to a circular cylinder in cross flow," *J. Heat Transfer Trans. ASME*, Ser. C, vol. 99, pp. 300–306, 1977.
[11] H. S. Carslaw and J. C. Jaeger, *Conduction of Heat in Solids*, 2nd ed. Oxford, U.K.:Clarendon Press, 1959.
[12] H. Brenner, "Forced convection heat and mass transfer at small Peclet numbers from a particle of arbitrary shape," *Chem. Eng. Sci.*, vol. 108, pp. 109–122, 1963.
[13] A. J. W. Dawkins, N. R. V. Nightingale, G. P. South, R. J. Sheppard, and E. H. Grant, "The role of water in microwave absorption by biological material with particular reference to microwave hazards," *Phys. Med. Biol.*, vol. 24, pp. 1168–1176, 1979.
[14] M. Kohli, W. N. Nei, E. W. Prohofsky, and L. L. Van Zandt, "Calculated microwave absorption of double-helical B-conformation Poly(dG)·Poly(dC)," *Biopolymers*, vol. 20, pp. 853–864, 1981.
[15] A. W. Friend, S. L. Gartner, K. R. Foster, and H. Howe, Jr., "The effects of high power microwave pulses on red blood cells and the relationship to transmembrane thermal gradients," *IEEE Trans. Microwave Theory Tech.*, to be published.

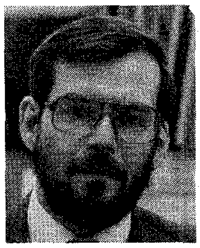

Kenneth R. Foster (M'76–SM'81) was born in Baltimore, MD in 1945. He received the Ph.D. in physics from Indiana University in 1971, and subsequently served as a Lieutenant, Medical Service Corps, U.S. Navy, at the Naval Medical Research Institute, Bethesda, MD.

Since 1976, he has been with the Department of Bioengineering of the University of Pennsylvania. He is currently an Assistant Professor and Undergraduate Curriculum Chairman of Bioengineering. His research interests are in the fields of mechanisms of interaction between nonionizing radiation and biological systems, electrical properties of heterogeneous systems, and microwave heating of tissues. He is a registered Professional Engineer in Pennsylvania.

Portonovo S. Ayyaswamy was born in 1942 in Bangalore, India. He received the Ph.D. in mechanical engineering in 1971 from the University of California at Los Angeles.

From 1971 until 1974 he was a postdoctoral scholar at UCLA, after which he joined the faculty at the University of Pennsylvania. He is currently Associate Professor in the Department of Mechanical Engineering. His research interests are in the fields of heat and mass transfer, with particular emphasis on convective heat transfer.

Dr. Ayyaswamy is the recipient of two University of Pennsylvania awards for excellence in teaching, and the Outstanding Faculty Advisor Award of the ASME. He is at present writing a book on heat and mass transfer.

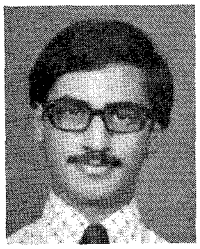

Thirumalchari Sundararajan was born in Madurai, India, in 1956. He received the B. Tech. degree from the Indian Institute of Technology in 1978, and the M.S. degree from the University of Pennsylvania in 1980. He is currently a Ph.D. candidate at the University of Pennsylvania, where he is doing research in the fields of heat transfer and fluid mechanics.

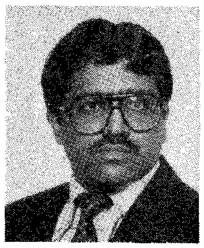

Koneru Ramakrishna was born in Pradesh, India, in 1954. He received the B.E. degree from Andhra University in 1976, the M. Tech. degree from the Indian Institute of Technology in 1978, and the M.S. degree from Kansas State University in 1980. He is currently a Ph.D. candidate at the University of Pennsylvania, where he is doing research in the fields of heat transfer and fluid mechanics.